Finite Element Model Updating of a Cable-Stayed Bridge Using Structural Health Monitoring Data

Thomas Sharry[1], Hong Guan[2], Nam Hoang[3], Andy Nguyen[4], Erwin Oh[5]
[1]PhD candidate, School of Engineering and Built Environment, Griffith University, Australia
[2]Professor, School of Engineering and Built Environment, Griffith University, Australia
[3]Associate Professor, University of Management and Technology, HCMC, Vietnam
[4]Senior Lecturer, School of Civil Engineering and Surveying, University of Southern Queensland, Australia
[5]Associate Professor, School of Engineering and Built Environment, Griffith University, Australia
email: thomas.sharry@griffithuni.edu.au, h.guan@griffith.edu.au, nam.hoang@umt.edu.vn, andy.nguyen@usq.edu.au, y.oh@griffith.edu.au

ABSTRACT This paper presents a finite-element model of the Phu My Bridge, a 380m-main span reinforced concrete cable-stayed bridge in Ho Chi Minh City, Vietnam. The model is also updated based on accelerometer data from the on-structure sensing system for structural health monitoring (SHM). A comprehensive sensitivity study is undertaken to examine the effects of various structural parameters on the modal properties, according to which a set of structural parameters are then selected for model updating. The finite-element model is updated in an iterative procedure to minimise the differences between the analytical and measured natural frequencies. The model updating process converges after a small number of four iterations, due to the accuracy of the initial model which was achieved through careful consideration of the structural parameter values for the model, optimal element discretisation for mesh convergence, and the most sensitive parameters for updating. The updated finite-element model for the Phu My Bridge is able to reproduce natural frequencies in good agreement with measured ones and can be helpful for long-term monitoring efforts.

KEY WORDS: Structural Health Monitoring; Sensitivity-Based Model Updating; Operational Modal Analysis.

1 INTRODUCTION

The Phu My Bridge (Figure 1), opened to traffic in 2009 and located over the Saigon River in Ho Chi Minh City (HCMC), Vietnam, is a critical link in the highway system around HCMC designed to relieve traffic congestion in the urban core. Additionally, the Phu My Bridge is an important link in the transport corridor from the southern Mekong Delta region to the central and northern parts of Vietnam. To ensure the structural integrity and operational safety, in 2019 the bridge was fitted with a structural health monitoring (SHM) sensing system that includes three inclinometers on the eastern side pylon, eight accelerometers (4 on the eastern deck and 4 on the four longest mid-span cables on the eastern side), one weather station, and one anemometer.

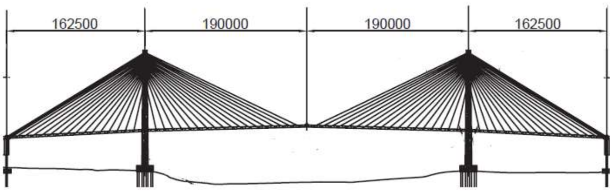

Figure 1. Phu My Bridge Layout.

A three-dimensional finite-element (FE) model was constructed using linear elastic beam elements for the deck, towers, and piers, truss elements for the cables, and elastic or rigid links for the connections and boundary constraints. The bridge deck girder, which is composed of two longitudinal concrete girders linked by transverse prestressed concrete cross girders at 5m intervals, is modelled using a single spine passing through the centre of the deck. The cables are modelled using single linear elastic truss elements and the nonlinear effect due to cable tension and sag is considered by linearizing the cable stiffness using an equivalent modulus of elasticity [1]. As this is the first attempt at updating the model with one set of data, for simplicity one value for the cable elastic modules is adopted for all cables. The FE model, after a mesh convergence study, consists of 2290 beam elements, 144 truss elements, and 2310 nodes as shown in Figure 2.

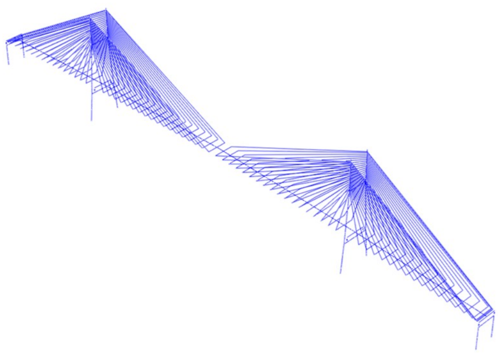

Figure 2. Three-dimensional model of Phu My Bridge.

2 METHODOLOGY

2.1 *Operational Modal Analysis*

Through Operational Modal Analysis (OMA), modal properties were identified from ambient vibration data captured by the Phu My SHM system over a seven-day period from July 29th to August 4th 2020. This was carried out by using two different output-only techniques: the Enhanced Frequency Domain Decomposition (EFDD) in the frequency domain and the data driven Stochastic Subspace Identification (SSI); these techniques are available in the commercial program ARTeMIS.

2.2 Finite Element Analysis

Modal properties identified from OMA show reasonable correlation with the FE model results in terms of natural frequencies and mode shapes. However, consistent discrepancies can be seen between the analytical and measured natural frequency results. While the finite element method is a mature technique, FE models are unable to predict structural responses with complete accuracy due to inherent errors in the modelling procedure. Errors that may cause discrepancies are well documented in the literature. Possible sources are [2]: (1) Structural modelling errors such as ill-defined boundary conditions, difficulty in modelling detailed, complex shapes, connections, joints, and assumptions for simplification purposes; (2) Structural parameter errors such as estimating values for unknown material properties; and (3) Model order errors resulting from inaccurate model discretisation. In this study, (1) and (2) are the major contributors of differences between the analytical and measured results.

2.3 Model Updating

If the measured modal properties identified from the SHM data are assumed to be very close to the actual behaviour of the structure, then the intent is to update the FE model so that the predicted modal properties match those obtained from measurements. This presents a challenging problem as complex structures with a large number of degrees of indeterminacy, such as cable-stayed bridges, have inherent uncertainties in many parameters and boundary conditions. Numerous model updating methods have been proposed to meet this challenge [3][4][5].

For cable-stayed bridges, the most popular updating methods are sensitivity-based and iterative i.e. changing the most sensitive model parameters iteratively until agreement between predicted and measured results has been achieved. This approach has the advantages of identifying parameters that can directly affect the modal properties of the structure and acquire an immediate physical interpretation of the updated results.

In this paper, a sensitivity-based updating method is used for updating the FE model of the Phu My Bridge. The method is based on the eigenvalue sensitivity of selected structural parameters that are assumed to fall within certain limits according to the degrees of uncertainty, possible variation, and engineering judgement. The changes of these parameters are found by minimising an objective function by solving a quadratic programming problem detailed in the next section.

3 SENSITIVITY-BASED PARAMETRIC UPDATING WITH CONSTRAINTS

As the relationship between the natural frequencies and model parameters is nonlinear, the problem is linearized and can be expressed as a Taylor series expansion (limited to the first two terms) [5]. Since the Taylor expansion is truncated by neglecting the higher-order terms, the shortened expansion necessitates several iterations. When very large discrepancies exist between the measured and analytical responses, the validity of the Taylor series truncations to first order is undermined and the iterative process is prone to divergence. As such, the initial FE model prior to updating should be relatively close to the measured behaviour [6].

The model updating approach adopted for this study utilises an improved sensitivity-based updating algorithm as described in [7]. This updating approach has the advantage of considering uncertainties in the measurements and the input parameters by utilizing weighting matrices. The formulation of the procedure is as follows.

The ith eigenvalue λ_i and the corresponding eigenvector ϕ_i of an undamped continuous system discretised into an n degrees of freedom FE model are obtained by solving the following eigenequation:

$$\mathbf{K}\Phi_i = \lambda_i \mathbf{M}\Phi_i \tag{1}$$

where $\mathbf{K}$ and $\mathbf{M}$ are the structural stiffness and mass matrices, respectively.

If from an initial FE model the set of structural parameters ($p_{i,a}$, $i = 1, 2, 3,\ldots\ldots, n_p$) can be represented by a vector $\mathbf{P}_a$

$$\mathbf{P}_a = [p_{i,a} \mid i = 1,2,3,\ldots\ldots.., n_p]^T \tag{2}$$

where n_p is the total number of structural parameters, then a set of eigenvalues ($\mathbf{\Lambda}_a$) can be obtained from the model as

$$\mathbf{\Lambda}_a = [\lambda_{i,a} \mid i = 1,2,3,\ldots\ldots.., n_a]^T \tag{3}$$

where n_a is the total number of computed modes. The subscript a in Eqs. (2) and (3) is used to indicate the results from the analytical model.

From SHM modal analysis of the structure, the modal characteristics of the structure can be determined and expressed as

$$\mathbf{\Lambda}_e = [\lambda_{i,e} \mid i = 1,2,3,\ldots\ldots.., n_e]^T \tag{4}$$

where $\mathbf{\Lambda}_e$ is the vector of measured eigenvalues, and n_e is the total number of measured modes. The subscript e is used to indicate that the properties are obtained from measurements. It may be assumed that the total number of measured modes is the same as the total number of analytical modes ($n_e = n_a$).

As mentioned previously, the analytical ($\mathbf{\Lambda}_a$) and the measured ($\mathbf{\Lambda}_e$) modal properties are usually discrepant due to inaccuracies in both the FE model and the measurements. For SHM purposes, it is assumed that the measured modal properties are very close to the actual behaviour of the structure and that the FE model errors are the main contributor to the discrepancy. Therefore, the model can be improved by the parametric model updating procedure. Let $\mathbf{P}_u$ represent the vector of structural parameters after updating

$$\mathbf{P}_u = [p_{i,u} \mid i = 1,2,3,\ldots\ldots.., n_p]^T \tag{5}$$

The relationship between the measured and initial model eigenvalues can be approximated by a first-order Taylor series expansion with respect to the structural parameters. The higher-order terms in the Taylor series expansion are neglected under the assumption that the changes in the structural parameters between successive iterations are sufficiently small:

$$\boldsymbol{\delta\Lambda} = \mathbf{S}\boldsymbol{\delta}\mathbf{P} \tag{6}$$

where $\boldsymbol{\delta\Lambda}$ is the eigenvalue residual vector calculated by $\boldsymbol{\Lambda}_e$ - $\boldsymbol{\Lambda}_a$; $\boldsymbol{\delta}\mathbf{P}$ is the perturbation vector of the structural parameters calculated by $\mathbf{P}_u$ - $\mathbf{P}_a$; and $\mathbf{S}$ is the sensitivity matrix.

As Eq. (6) attempts to determine the change in parameters required to obtain the measured observations, Eq. (6) is formulated as an inverse problem. The selection of updating parameters depends on their sensitivity, and the total number of updating parameters determines the complexity of the optimisation problem. Therefore, reducing this number by determining the most sensitive parameters is critical to successful model updating. A sensitivity analysis for each parameter computes the sensitivity coefficient defined as the rate of change of a particular response quantity with respect to a change in the structural parameter. For all selected responses and parameters, the sensitivity matrix $\mathbf{S}_{ij}$ with respect to eigenvalues is obtained by [8]:

$$\mathrm{S_{ij}} = \frac{\delta\lambda_i}{\delta P_j} \tag{7}$$

where δP_j and $\delta\lambda_i$ are the change in parameter and the corresponding change in response, respectively. If sensitivities for different types of parameters are to be compared, then the relative sensitivity matrix $\mathbf{S}_r$ is defined by [6]:

$$\mathrm{S_{r_{ij}}} = \left(\frac{\delta\lambda_i}{\delta P_j}\right) P_j \tag{8}$$

where $\mathbf{P}_j$ is the structural parameters evaluated either at the initial estimate $\mathbf{P}_a$, or at an iteration value during the updating process where $j = 1, 2, 3, \ldots, n$ for n iterations.

The relative sensitivities can be also normalised with respect to the response value to form the normalised sensitivity matrix $\mathbf{S}_n$ defined by:

$$\mathrm{S_{n_{ij}}} = \left(\frac{\delta\lambda_i}{\delta P_j}\right) \cdot \left(\frac{P_j}{\lambda_i}\right) \tag{9}$$

The following objective function was proposed to solve the inverse problem as stated in Eq. (6) [9].

$$\mathbf{J} = \boldsymbol{\delta}\mathbf{P}^{\mathbf{T}}\mathbf{W_P}\boldsymbol{\delta}\mathbf{P} + (\mathbf{S}\boldsymbol{\delta}\mathbf{P} - \boldsymbol{\delta\Lambda})^{\mathbf{T}}\mathbf{W_E}(\mathbf{S}\boldsymbol{\delta}\mathbf{P} - \boldsymbol{\delta\Lambda}) \tag{10}$$

where $\mathbf{W_P}$ and $\mathbf{W_E}$ are the positive definite weighting matrices. $\mathbf{W_P}$ is chosen to restrain large changes to more certain parameters or parameters that may affect the eigenvalues drastically, and $\mathbf{W_E}$ is chosen to give weighting to those eigenvalues that are more certain than others.

To avoid very large variations in parameter perturbation that violate the assumption of the first-order Taylor series approximation and reduce the physical meaning of the updated result, inequality constraints for each structural parameter are implemented as follows:

$$\mathbf{B}_l \leq \mathbf{P} \leq \mathbf{B_u} \tag{11}$$

$$\mathbf{b}_l \leq \boldsymbol{\delta}\mathbf{P} \leq \boldsymbol{b}_\mathbf{u} \tag{12}$$

where $\mathbf{B_l}$ and $\mathbf{B_u}$ are vectors of lower and upper bounds for the structural parameters $\mathbf{P}$, respectively, and $\mathbf{b_l}$ and $\mathbf{b_u}$ are vectors of lower and upper bound perturbations for the change in structural parameters $\boldsymbol{\delta}\mathbf{P}$, respectively.

Figure 3 presents an overview of the model updating procedure to solve Eq. (6).

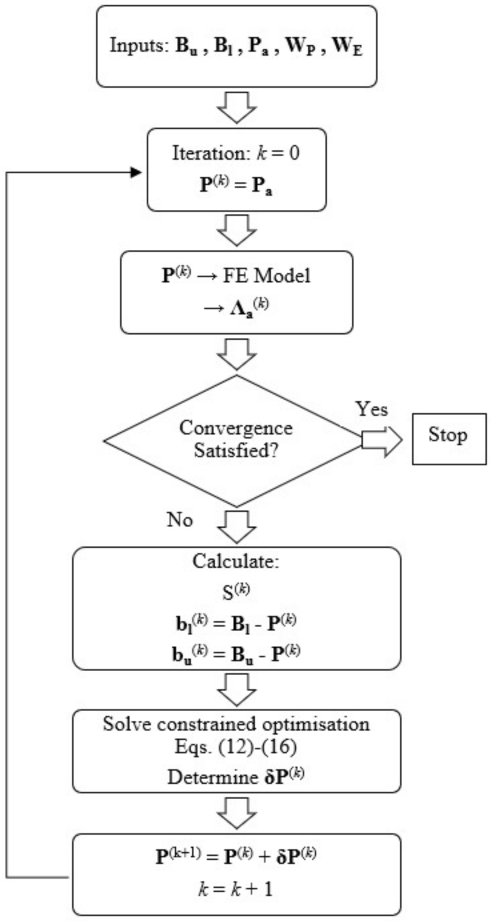

Figure 3. Flowchart sensitivity-based model updating with constraints [7].

Thus, parameter updating can now be achieved by minimising the objective function (Eq. (10)) subjected to the constraints defined by Eq. (11). This constrained optimisation may be stated as the following quadratic programming problem: Minimise

$$\mathbf{J}(\mathbf{x}) = {}^{\mathbf{1}}\!/_{\mathbf{2}}\, \mathbf{x}^{\mathbf{T}}\mathbf{W}\mathbf{x} \tag{13}$$

subject to:
$\mathbf{A}_i\mathbf{x} = \mathbf{d}_i$ ($i = 1, 2, 3, \ldots, n_e$) and
$\mathbf{A}_i\mathbf{x} \leq \mathbf{d}_i$ ($i = n_e + 1, n_e + 2, n_e + 3, \ldots, n_e + 2n_p$)

where

$$\mathbf{x} = \begin{Bmatrix} \boldsymbol{\delta}\mathbf{P} \\ \mathbf{S}\boldsymbol{\delta}\mathbf{P} - \boldsymbol{\delta}\boldsymbol{\Lambda} \end{Bmatrix} \tag{14}$$

$$\mathbf{d} = \begin{Bmatrix} \boldsymbol{\delta}\boldsymbol{\Lambda} \\ \mathbf{b}_u \\ -\mathbf{b}_l \end{Bmatrix} \tag{15}$$

$$\mathbf{A} = \begin{bmatrix} \mathbf{S} & -\mathbf{I} \\ \mathbf{I} & \mathbf{0} \\ -\mathbf{I} & \mathbf{0} \end{bmatrix} \tag{16}$$

$$\mathbf{W} = \begin{bmatrix} \mathbf{W}_P & \mathbf{0} \\ \mathbf{0} & \mathbf{W}_E \end{bmatrix} \tag{17}$$

and $\mathbf{A}_i$ and $\mathbf{d}_i$ refer to the ith row of matrix **A** and vector **d**, respectively.

4 SELECTION OF MATCHING MODES AND UPDATING PARAMETERS

Before updating the model, the modes are selected for matching between the FE analysis results and the OMA measurements, and the structural parameters selected to be included for updating. It would be ideal if as many modes as possible are matched between the analytical predictions and measurements. However, it is generally assumed that the identification of lower modes is more reliable than higher modes and therefore focusing on matching lower modes is more logical. In this study, the lowest 15 modes with frequencies ranging between 0.2 and 1.2 Hz identified from the initial model are chosen to be matched with the OMA results. These include eight vertical-dominant, one lateral-dominant, one torsional-dominant, and one longitudinal-dominant modes of the deck. The frequencies determined from the initial FE model and their corresponding values obtained from OMA measurements are summarised in Table 1. Note that modes 4, 5, 12 and 13 identified from the FE results were not identified from the OMA.

A comprehensive eigenvalue sensitivity analysis is performed to study the effects of parameters on the selected mode frequencies. These parameters include geometry and material properties of the deck, towers, material properties of the cables, as well as the boundary conditions of the deck/pylon and deck/pier connections (Table 2). Some key considerations associated with the parameter updating and sensitivity analysis are summarised as follows:

1. For description purposes, the structural parameters are grouped into geometry, non-structural mass, and materials.
2. For reference purposes, the pylons have been divided into five distinct parts as shown in Figure 4.
3. It is assumed that the cross sections of the deck, pylons, and piers have homogeneous properties that do not vary.
   The parameterisation of the connections and boundary conditions present a challenge to defining the initial model, and to model updating. In this study, three elastic springs with one, two, and three degrees of freedom (DOF) respectively are assigned to each deck/pylon and deck/pier connection. This DOF combination of elastic springs allows suitable mode shape behaviour with any 'separation' between deck and pylon, and deck and pier. The pylon and pier legs are fully fixed to the ground.

Table 1. Selected modes for model updating.

#	Mode shape description	Notat-ion	FE Model (Hz)	OMA (Hz)	% diff.
1	First vertical bending of deck	VD1	0.260	0.281	-7.40
2	Second vertical bending of deck	VD2	0.346	0.362	-4.42
3	First lateral bending of deck	LD1	0.425	0.428	-0.64
4	First lateral mode of towers	LT1	0.515	-	-
5	Second lateral mode of towers	LT2	0.520	-	-
6	Third vertical bending of deck	VD3	0.521	0.554	-6.05
7	Fourth vertical bending of deck	VD4	0.580	0.614	-5.52
8	First longitudinal bending of deck + towers	LDT1	0.621	0.665	-6.55
9	Fifth vertical bending of deck	VD5	0.677	0.684	-1.06
10	First torsional mode of deck	TD1	0.830	0.836	-0.75
11	Sixth vertical bending of deck	VD6	0.891	0.899	-0.85
12	First lateral mode of end piers	LP1	0.978	-	-
13	Second lateral mode of end piers	LP2	0.981	-	-
14	Seventh vertical bending of deck	VD7	1.071	1.163	-7.93
15	Eighth vertical bending of deck	VD8	1.127	1.21	-6.83

Note: % diff. = (Initial FE model results – OMA results) / OMA results

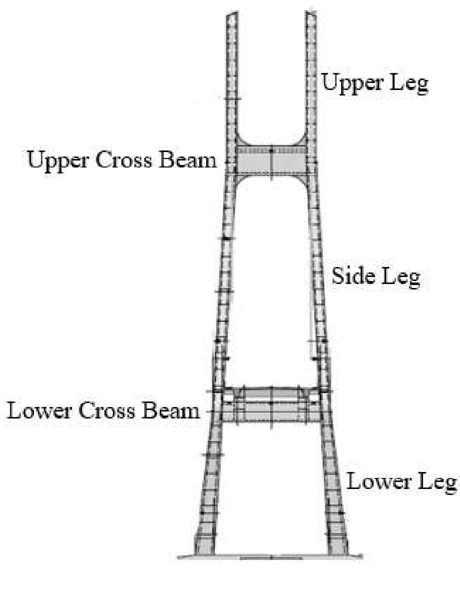

Figure 4. Pylon definitions.

Table 2. Model input parameters.

Index	Parameters	Initial estimation
	Geometry Parameters	
G1	Pylon lower leg cross sectional area	35 m^2
G2	Pylon side leg cross sectional area	18 m^2
G3	Pylon upper leg cross sectional area	15 m^2
G4	Pylon lower cross beam (CB) cross sectional area	30 m^2
G5	Pylon upper cross beam (CB) cross sectional area	25 m^2
G6	End pier leg cross sectional area	15 m^2
G7	End pier cross beam (CB) cross sectional area	6 m^2
G8	Girder cross sectional area	23 m^2
G9	Girder moment of inertia (I)	21 m^4
G10	Girder torsional inertia (I)	58 m^4
G11	Stay cable cross sectional area	Varied
	Non-structural Parameters	
NS12	Non-structural (NS) girder mass	15000 kg/m
	Material Parameters	
M13	Pylons and piers concrete strength	60 MPa
M14	Girder concrete strength	60 MPa
M15	Stay cable Young's modulus (E)	195 GPa
M16	Concrete density	2500 kg/m^3
M17	Stay cable density	7850 kg/m^3
M18	Concrete Poisson's ratio	0.2
M19	Stay cable Poisson's ratio	0.3
M20	Spring stiffness	3 x 10^7 N/m

The eigenvalue sensitivities of the 15 selected modes with respect to all parameters described above are computed using Eq. (9). This dimensionless sensitivity indicates the effect of a certain parameter on a particular frequency. The sensitivities range between -0.4 and 0.4. Table 3 lists the input parameters from the most sensitive to the least sensitive and noting their sensitivity effect - positive sign indicates that an increase in parameter values results in an increase in natural frequencies, and negative sign indicates an increase in parameter values results in a decrease in natural frequencies.

Table 3. Model input parameters from most sensitive to least.

Rank	Index	Parameter	Sensitivity effect
1	M16	Concrete density	-
2	M15	Stay cable Young's modulus (E)	+
3	G8	Girder cross sectional area	-
4	G11	Stay cable cross sectional area	+
5	G2	Pylon side leg cross sectional area	+
6	G1	Pylon lower leg cross sectional area	+/-
7	M13	Pylons and piers concrete strength	+
8	G9	Girder moment of inertia (I)	+
9	M14	Girder concrete strength	+
10	NS12	Non-structural (NS) girder mass	-
11	G3	Pylon upper leg cross sectional area	+/-
12	M17	Stay cable density	-
13	G4	Pylon lower cross beam (CB) cross sectional area	+
14	G5	Pylon upper cross beam (CB) cross sectional area	+/-
15	G10	Girder torsional inertia (I)	+
16	G6	End pier leg cross sectional area	+/-
17	M20	Spring stiffness	-
18	G7	End pier cross beam (CB) cross sectional area	No effect
19	M18	Concrete Poisson's ratio	No effect
20	M19	Stay cable Poisson's ratio	No effect

5 PARAMETER UPDATING AND UPDATED MODEL RESULTS

To reduce the complexity of model updating, only those parameters with higher sensitivity and with a reasonable degree of uncertainty are included and listed in Table 4. Since the geometry of the cables are well documented, the cross-sectional areas of the stay cables are assumed to be correct and are excluded as candidate parameters for adjustment. Additionally, the least sensitive parameters are also excluded.

Table 4. Model input parameters selected for adjustment.

Index	Parameter
M16	Concrete density
M15	Stay cable Young's modulus (E)
G1	Pylon lower leg cross sectional area
G2	Pylon side leg cross sectional area
G3	Pylon upper leg cross sectional area
G4	Pylon lower cross beam (CB) cross sectional area
G5	Pylon upper cross beam (CB) cross sectional area
G8	Girder cross sectional area
G9	Girder moment of inertia (I)
NS12	Non-structural (NS) girder mass
M14	Girder concrete strength
M13	Pylons and piers concrete strength

The structural parameters in Table 4 are updated in an iterative fashion using the procedure illustrated in Figure 3. The initial estimates of the parameters used in the initial finite-element model as listed in Table 2 are taken as the starting point for the iterative process. For each iteration, an eigenvalue sensitivity analysis is preformed using the parametric values updated in the previous iteration. The parameters are restrained from extreme changes in each iteration by choosing a weighting matrix $\mathbf{W_P}$ so as not to violate the first-order Taylor series expansion approximation for Eq. (6).

The 12 most sensitive structural parameters in Table 4 are updated gradually in each iteration with the natural frequencies calculated at the end of each iteration gradually approaching those of the measured values. The convergence criterion used to stop the iteration is set to ± 4.5% difference between the measured and calculated frequencies across all modes (Table 5).

The convergence of the updating process is reached after four iterations. Table 5 summarises the 15 frequencies calculated during these four iterations. Most of the calculated frequencies converge gradually toward the corresponding measured values. The differences between the measured and calculated frequencies for the initial and final (4th iteration) updated models are plotted in Figure 5. The updated model frequencies are generally closer to the measured frequencies and the updated results fall within ±4.5%. However, as shown in Figure 5, the frequency differences of modes 9 and 11 increase as the iteration increases. This is attributed to the fact that global fitting of frequencies can sacrifice the matching of some individual modes.

Table 5. Model updating results.

Mode	Finite-Element model frequency results (Hz): Initial model	Updated model after iteration: 1st	2nd	3rd	4th
VD1	0.260	0.265	0.269	0.272	0.273
VD2	0.346	0.352	0.358	0.361	0.364
LD1	0.425	0.426	0.427	0.428	0.428
LT1	0.515	0.514	0.513	0.511	0.510
LT2	0.520	0.519	0.518	0.516	0.515
VD3	0.521	0.545	0.549	0.550	0.550
VD4	0.580	0.595	0.601	0.607	0.609
LDT1	0.621	0.631	0.638	0.640	0.642
VD5	0.677	0.685	0.699	0.710	0.712
TD1	0.830	0.829	0.829	0.828	0.828
VD6	0.891	0.920	0.930	0.936	0.938
LP1	0.978	0.994	1.001	1.005	1.007
LP2	0.981	0.995	1.005	1.010	1.012
VD7	1.071	1.095	1.115	1.125	1.126
VD8	1.127	1.165	1.175	1.182	1.185

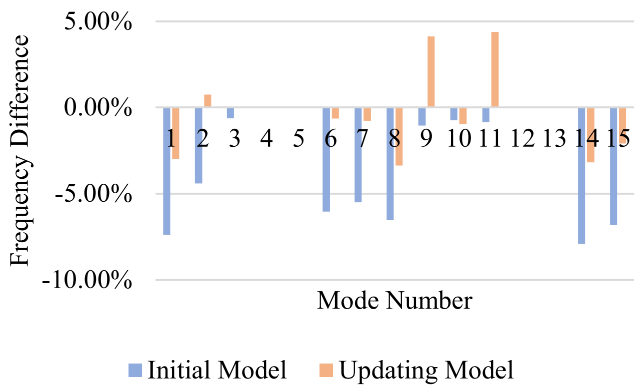

Figure 5. Comparison of frequency difference between initial and final (4th iteration) updated model.

Table 6 shows the updated values of the 12 structural parameters at the end of the 4th iteration as compared to the initial estimates. All show variations except for the pylon lower and upper cross beams which show very minor changes. The fact that the initial model being quite close to the measured values (<10% differences) means the changes in the parameter values are generally minor in nature. It should be acknowledged that there is no evidence to suggest that the updated structural parameter values are the 'true' values for the Phu My Bridge. The set of updated parameters can be considered plausible candidates among many sets of parameters with different combinations that can satisfy the constrained optimisation problem.

Further running of the updating procedure does not show reduced differences between the updated model and the OMA results. Modes 9 and 11 in particular continue to increase in difference between the updated model and the measured results. If modes 9 and 11 are excluded and the iterations continued, only a minor improvement is achieved, and additional iterations cannot reduce the frequency differences further. This is attributed to errors associated with collecting and postprocessing the measurement data, the simplifications and assumptions in the FE model, and the inherent assumptions and limitations of the presented updating procedure.

Table 6. Updated parameter values.

Index	Parameter	Initial estimation	Updated value
M16	Concrete density (kg/m^3)	2500	2507
M15	Stay cable Young's modulus (E) (GPa)	195	194.95
G1	Pylon lower leg cross sectional area (m^2)	35	35.1
G2	Pylon side leg cross sectional area (m^2)	18	18.4
G3	Pylon upper leg cross sectional area (m^2)	15	15.5
G4	Pylon lower cross beam (CB) cross sectional area (m^2)	30	30.02
G5	Pylon upper cross beam (CB) cross sectional area (m^2)	25	25.01
G8	Girder cross sectional area (m^2)	23	20.5
G9	Girder moment of inertia (I) (m^4)	21	21.7
NS12	Non-structural (NS) girder mass (kg/m)	15000	14987
M14	Girder concrete strength (MPa)	60	55
M13	Pylons and piers concrete strength (MPa)	60	55

6 CONCLUSION

This paper presents the first attempt of dynamic modelling and model updating of the Phu My Bridge. A total of 15 modes, with a frequency range between 0.2 and 1.2 Hz, are selected for matching between the measured and calculated FE results. A total of 12 structural parameters are selected for updating based on an eigenvalue sensitivity study. The updating method used is an eigenvalue sensitivity-based approach, and the parameters are bounded according to their degree of uncertainty and possible variation based on engineering judgement. The model updating process converges after a small number of four iterations. The small number of iterations highlights the importance of accurate initial modelling in reducing the computational demand and complexity of the updating problem. Accurate modelling was achieved through careful consideration of the structural parameter values for the model, optimal element discretisation for mesh convergence, and the most sensitive parameters for updating. Overall, the frequencies calculated from the updated model are closer to the measured values when compared to those calculated from the initial model.

This study summarises the updating of an initial FE model based on on-structure sensing system and SHM vibration data. The results suggest that it is possible to use bridge SHM data to update a FE model so that the numerical natural frequencies are reasonably close to the measured ones. Complete elimination of the frequency differences, however, presents challenges due to inherent assumptions introduced before and during the formation of the model updating process.

REFERENCES

[1] J. Ernst, *Der E-Modul von Seilen unter berucksichtigung des Durchhanges,* Der bauingerieur, 40(2), 53-55, (1965).

[2] J.E. Mottershead and M. Friswell, *Model updating in structural dynamics: a survey*, Journal of Sound and Vibration, 167(2), 347-375, (1993).

[3] S. Sehgal and H. Kumar, *Structural dynamic model updating techniques: A start of the art review*, Archives of Computational Methods in Engineering, 23(3), 515-533, (2016).

[4] T. Marwala, *Finite element model updating using computational intelligence techniques: applications to structural dynamics*, Springer Science & Business Media, (2010).

[5] M. Friswell and J.E. Mottershead, *Finite element model updating in structural dynamics*, Vol. 38, Springer Science & Business Media, (2013).

[6] J.M. Brownjohn, P.Q. Xia, H. Hao and Y. Xia, *Dynamic assessment of curved cable-stayed bridge by model updating*, Journal of structural engineering, 126(2), 253-260, (2001).

[7] Q. Zhang, T.Y.P. Chang and C.C. Chang, *Finite-element model updating for the Kap Shui Mun cable-stayed bridge*, Journal of bridge engineering, 6(4), 285-293, (2001).

[8] J.M. Brownjohn and P.Q. Xia, *Dynamic assessment of curved cable-stayed bridge by model updating*, Journal of structural engineering, 126(2), 252-260, (2000).

[9] M. Link and Z. Qian, *Updating substructure models with dynamic boundary conditions*, Paper presented at the 1995 Des. Engrg. Tech. Conf., (1995).